Journal of Alloys and Compounds 509 (2011) 1744–1748

Contents lists available at ScienceDirect

Journal of Alloys and Compounds

journal homepage: www.elsevier.com/locate/jallcom

Electrical characteristics of $Li(Ni_{7/10}Fe_{3/10})VO_4$ ceramics

Moti Ram*

Department of Physics and Meteorology, Indian Institute of Technology, Kharagpur, West Bengal 721302, India

ARTICLE INFO

Article history:
Received 5 June 2010
Received in revised form
27 September 2010
Accepted 28 September 2010
Available online 19 October 2010

Keywords:
Ceramics
Solution-based chemical method
Complex impedance spectroscopy

ABSTRACT

The compound $[Li(Ni_{7/10}Fe_{3/10})VO_4]$ was produced by a solution-based chemical route whose electrical properties were investigated using complex impedance spectroscopy technique. X-ray diffraction study reveals an orthorhombic unit cell structure of the compound. Complex electrical impedance analysis exhibits: (i) grain interior, grain boundary and electrode-material interface contributions to electrical response and (ii) the presence of temperature dependent electrical relaxation phenomena in the material. Electrical conductivity study indicates that electrical conduction in the material is a thermally activated process.

1. Introduction

Recently, lithiated transition metal oxides have attracted large academic and technological attention [1–9]. It is due to the potential applications in several industrial fields such as superconductors [1,2,10,11], cathodes for rechargeable lithium battery [3–5,12,13], humidity sensors [14,15] and so on. These oxides exhibit unique physical (electrical, magnetic, etc.) and chemical properties. The electronic nature of these oxides gives information about electrical behavior and it may be related to structural/microstructural properties [16–18]. Complex impedance spectroscopy technique is used to study the electrical properties of such type of materials [18,19]. Material's response is interesting for its capacitive and resistive behaviors, which attribute to the bulk grains, grain boundaries or defects present at material–electrode interface and modeled by R–C parallel circuit, series combination of two R–C parallel circuits or series combination of three R–C parallel circuits, respectively [18–23]. Electrical properties of such type of oxides are studied by various researchers using complex impedance spectroscopy technique [24–34]. This has motivated me to prepare a lithiated transition metal oxide $[Li(Ni_{7/10}Fe_{3/10})VO_4]$ and study its electrical (complex electrical impedance and electrical conductivity) properties. The compound $[Li(Ni_{7/10}Fe_{3/10})VO_4]$ is mechanically strong and may be useful as electrode material. In the current paper, I present a study of electrical (complex electrical impedance and electrical conductivity) properties of the compound $[Li(Ni_{7/10}Fe_{3/10})VO_4]$ using an a.c. technique of complex impedance spectroscopy.

2. Experimental procedures

2.1. Material preparation

A solution-based chemical route was used to prepare a $Li(Ni_{7/10}Fe_{3/10})VO_4$ ceramics. The stoichiometric amounts of highly pure $LiNO_3$, $Ni(NO_3)_2{\cdot}6H_2O$, $FeCO_3$ and NH_4VO_3 were dissolved in distilled water and mixed together. $FeCO_3$ was dissolved in warm distilled water in the presence of oxalic acid. Thereafter triethanolamine was added maintaining a ratio of 3:1 with metal ions. HNO_3 and oxalic acid were added to dissolve the precipitate and then the clear solution was evaporated at temperature (~200 °C) with continuous stirring. A fluffy, mesoporous and carbon-rich precursor mass was formed by complete evaporation of the solution. After grinding, the voluminous, fluffy and black carbonaceous mass was calcined at 525 °C for 4 h to produce a desired phase, which is confirmed by X-ray diffraction analysis. The calcined powder was cold pressed into circular disc shaped pellet of diameter 12–13 mm and various thicknesses with polyvinyl alcohol as a binder using hydraulic press at a load of ~3–4 tonnes. These pellets were then sintered at 575 °C for 2 h followed by slow cooling process. Subsequently, the pellets were polished by fine emery paper to make their faces smooth and parallel. The pellets were finally coated with conductive silver paint and dried at 150 °C for 3 h before carrying out electrical measurements.

2.2. Material characterization

X-ray diffraction of the calcined powder was studied at room temperature using a diffractometer (PANalytical PW 3040/60 X'Pert PRO) in the angle range $20^\circ \leq 2\theta \leq 80^\circ$ on being irradiated by Cu Kα radiation of wavelength equal to 1.5419 Å. The surface morphology of the gold-sputtered sample is recorded with different magnifications at room temperature using a ZEISS (Model: SUPRA™ 40) field emission scanning electron microscope. Electrical impedance, phase angle, tangent loss and capacitance were measured by applying a voltage of ~0.701 V using a computer-controlled frequency response analyzer (HIOKI LCR Hi TESTER, Model: 3532-50) with varying temperature over the frequency range 10^2–10^6 Hz.

* Tel.: +91 3222 281902.
E-mail address: motiram05@yahoo.co.in

0925-8388/$ – see front matter © 2010 Elsevier B.V. All rights reserved.
doi:10.1016/j.jallcom.2010.09.212

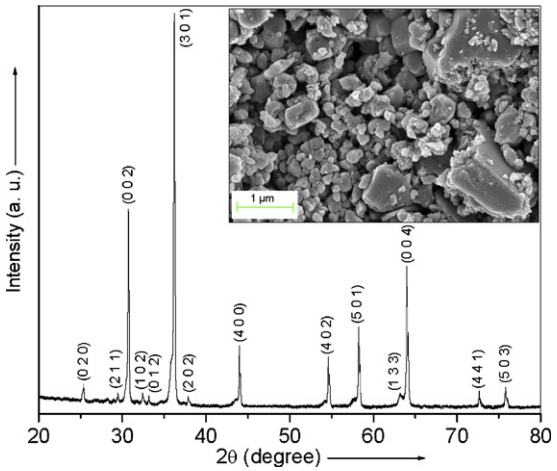

Fig. 1. X-ray diffraction pattern and field emission scanning electron micrograph (inset) of $Li(Ni_{7/10}Fe_{3/10})VO_4$ at room temperature.

3. Results and discussion

3.1. Structure/microstructure

Fig. 1 shows the X-ray diffraction pattern of the powder sample at room temperature, which reveals the formation of a single-phase compound. All reflection peaks of the X-ray profile are indexed and lattice parameters are determined using least-squares refinement method with the help of standard computer software (POWD MULT) [35]. An orthorhombic unit cell structure is selected on the basis of good agreement between observed and calculated interplaner spacing (d-values). The least-squares refined lattice parameters are $a = 8.2272$ Å, $b = 7.0230$ Å and $c = 5.8281$ Å. The values of the indexed peaks are given in Table 1. Clearly, $Li(Ni_{7/10}Fe_{3/10})VO_4$ prepared by solution-based chemical method results in modification of lattice parameters and its unit cell structure remains same for $LiFeVO_4$ and $LiFe_{1/2}Ni_{1/2}VO_4$ that were prepared by conventional solid state route [28,29]. But, the unit cell structure is changed to cubic for $LiNiVO_4$ that was prepared by solution-based chemical method [30].

The field emission scanning electron micrograph of the material's sintered pellet is shown in Fig. 1(inset). It indicates a polycrystalline texture of the compound with grains of unequal sizes (~0.1–1.6 μm). These grains present an average grain size with polydisperse distribution on the surface of the sample. The grain size (~0.1–1.6 μm) of $Li(Ni_{7/10}Fe_{3/10})VO_4$ is smaller than that of the grain size (~1–3 μm) of $LiFeVO_4$ and $LiFe_{1/2}Ni_{1/2}VO_4$ [28,29], and (~0.2–2.0 μm) of $LiNiVO_4$ [30], which indicates a clear modification in the microstructure of $LiFeVO_4$, $LiFe_{1/2}Ni_{1/2}VO_4$ and $LiNiVO_4$.

3.2. Complex electrical impedance

The variation of Z' (real part of electrical impedance) with Z'' (imaginary part of electrical impedance) at some selected temperatures is shown in Fig. 2. These are called the Nyquist plots and present semicircular arcs. The presence of single semicircular arc at 24 and 50 °C in the pattern indicates that electrical conduction in the material is due to the bulk effect, and it is modeled by a parallel R–C circuit. Double semicircular arcs at 75, 100, 200 and 225 °C show that electrical conduction in the material is due to the bulk and grain boundary effects, and modeled by a series combination of two parallel R–C circuits. Triple semicircular arcs are observed in the pattern at 250 and 275 °C, which indicate electrical conduction in the material is due to the bulk, grain boundary

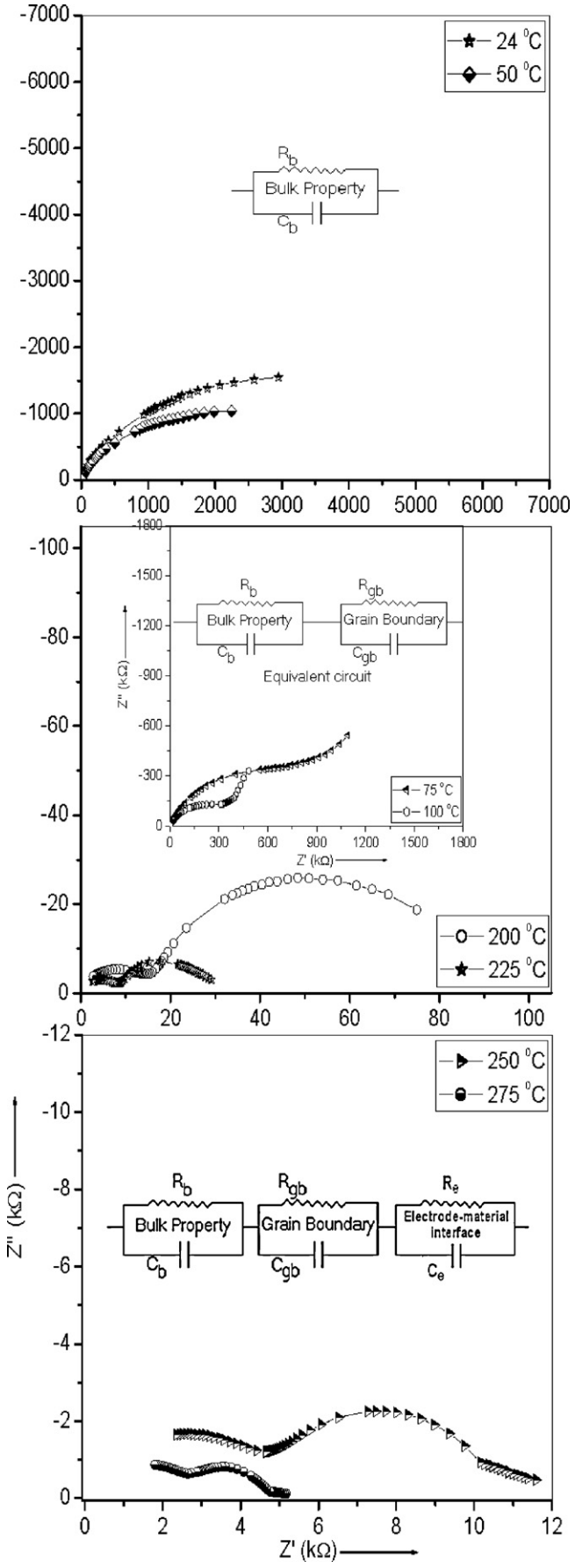

Fig. 2. Nyquist plots at some selected temperatures with electrical equivalent circuit (inset).

Table 1
X-ray diffraction data of $Li(Ni_{7/10}Fe_{3/10})VO_4$.

Diffraction angle 2θ (degree)	d-spacing (Å)		Miller indices			Rel. intensity (%)
	$d_{obs.}$	$d_{cal.}$	h	k	l	I/I_o
25.37	3.5108	3.5115	0	2	0	4.47
29.46	3.0316	3.0315	2	1	1	2.67
30.72	2.9107	2.9141	0	0	2	49.80
32.42	2.7614	2.7468	1	0	2	2.86
33.16	2.7018	2.6916	0	1	2	2.21
36.20	2.4815	2.4814	3	0	1	100.00
37.85	2.3768	2.3779	2	0	2	2.20
44.00	2.0578	2.0568	4	0	0	15.48
54.63	1.6799	1.6804	4	0	2	13.00
58.24	1.5841	1.5835	5	0	1	20.43
63.19	1.4715	1.4709	1	3	3	3.33
63.99	1.4550	1.4570	0	0	4	35.73
72.66	1.3012	1.3016	4	4	1	4.26
75.79	1.2551	1.2556	5	0	3	5.46

and polarization (polarization at the electrode–material interface) effects, and it is modeled by a series combination of three parallel R–C circuits [19]. But, electrical conduction in the material is due to the bulk effect at $T \leq 100\,^{\circ}C$ for $LiFeVO_4$, $T \leq 175\,^{\circ}C$ for $LiFe_{1/2}Ni_{1/2}VO_4$ and $T \leq 375\,^{\circ}C$ for $LiNiVO_4$, and due to the bulk and grain boundary effects at $125\,^{\circ}C \leq T \leq 250\,^{\circ}C$ for $LiFeVO_4$ and $200\,^{\circ}C \leq T \leq 350\,^{\circ}C$ for $LiFe_{1/2}Ni_{1/2}VO_4$ (i.e., electrical conduction in the material is due to the bulk effect in $LiNiVO_4$, and due to the bulk and grain boundary effects in $LiFeVO_4$ and $LiFe_{1/2}Ni_{1/2}VO_4$ at studied temperatures) [28–30]. That indicates a clear modification in the electrical behavior of $LiFeVO_4$, $LiFe_{1/2}Ni_{1/2}VO_4$ and $LiNiVO_4$. Furthermore, a decrease of arc's intercept on real axis with rise in temperature indicates a reduction in resistive behavior of the material (i.e., negative temperature coefficient of resistance (NTCR) behavior of the material).

Fig. 3 shows frequency dependence of Z' at some selected temperatures. The value of Z' decreases with rise in both the frequency and temperature, which indicates an increase in conductivity. A merger of curves at high frequencies is due to the possible release of space charge [19,36]. Similar behavior was shown by $LiFeVO_4$, $LiFe_{1/2}Ni_{1/2}VO_4$ and $LiNiVO_4$ [28–30]. The frequency dependence of Z'' at some selected temperatures is shown in Fig. 4. It is observed that peaks with asymmetric broadening are shifting towards the high frequency side with rise in temperature. This suggests the presence of electrical relaxation process in the material with temperature dependence of relaxation time [36]. Also, asymmetric broadening of the peak with temperature-rise indicates non-unique (i.e., multiple) relaxation-timescale. Similar features were shown by $LiFeVO_4$, $LiFe_{1/2}Ni_{1/2}VO_4$ and $LiNiVO_4$ [28–30].

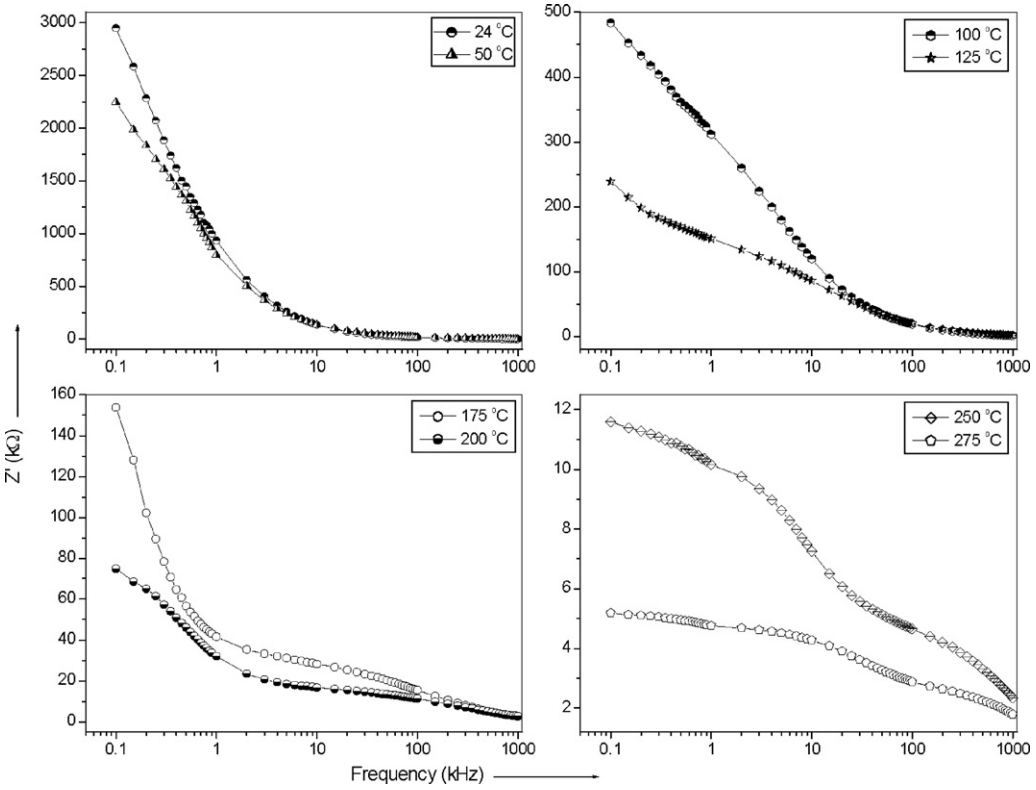

Fig. 3. Frequency dependence of Z' at some selected temperatures.

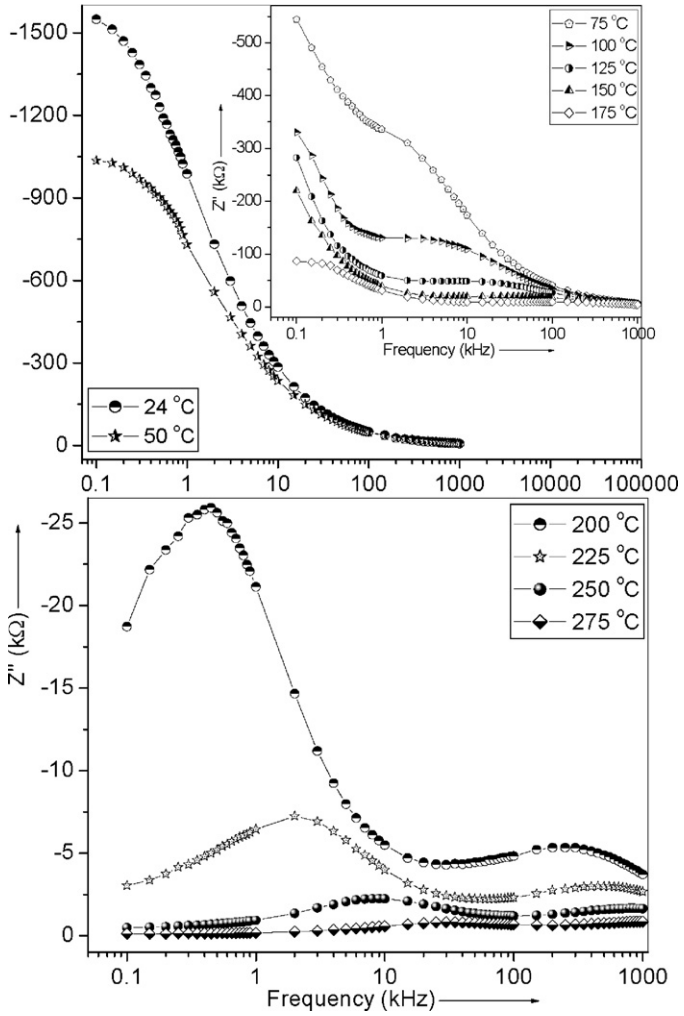

Fig. 4. Frequency dependence of Z'' at some selected temperatures.

3.3. Electrical conductivity

The variation of d.c. conductivity (σ_{dc}) with temperature is given in Fig. 5. The value of σ_{dc} increases with rise in temperature,

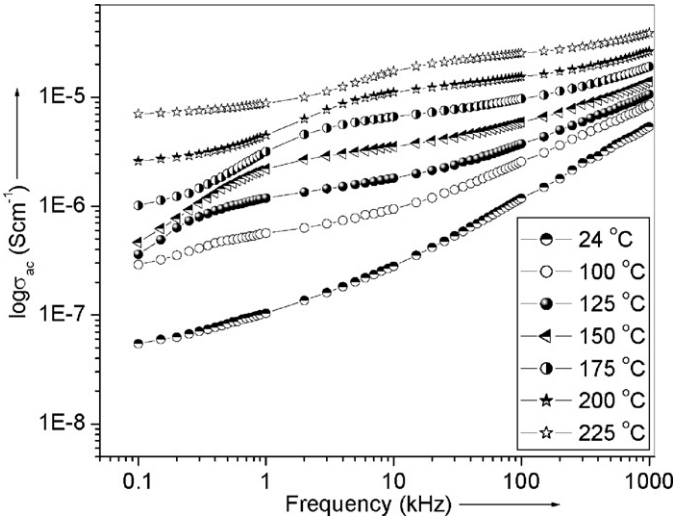

Fig. 6. Frequency dependence of σ_{ac} at some selected temperatures.

which follows a thermally activated Arrhenius relation [$\sigma_{dc} = \sigma_o \exp(-E_a/kT)$], where σ_o is the pre-exponential factor corresponding to $1/T = 0$, E_a is the activation energy for charge transfer, k is the Boltzmann constant and T is the absolute temperature [37]. This feature suggests that the electrical conduction in the material is a thermally activated process. Using the above Arrhenius relation and slope of Fig. 5, the activation energy (E_a) is calculated as ($\sim 0.488 \pm 0.003$ eV at 50–250 °C). Furthermore, E_a of $Li(Ni_{7/10}Fe_{3/10})VO_4$ is greater than that of E_a ($\sim$0.24 eV at 50–325 °C) of $LiFeVO_4$ [28], E_a ($\sim$0.42 eV at 23–350 °C) of $LiFe_{1/2}Ni_{1/2}VO_4$ [29] and E_a ($\sim$0.06 eV at 25–225 °C) of $LiNiVO_4$ [30]. This indicates a difference in the energy barrier for the charge carriers to overcome it [38].

Fig. 6 shows frequency dependence of a.c. conductivity (σ_{ac}) at some selected temperatures. It is observed that the value of σ_{ac} decreases with decrease in frequency and becomes independent of frequency after a certain value. Extrapolation of this part towards lower frequency will give σ_{dc}. This type of conduction behavior obeys the Jonscher's power equation [$\sigma(\omega) = \sigma_{dc} + A(\omega)^n$], where n is the frequency exponent in the range $0 \le n \le 1$ and A is a constant that depends upon temperature [39]. The increasing nature of σ_{ac} with temperature suggests that electrical conduction in the mate-

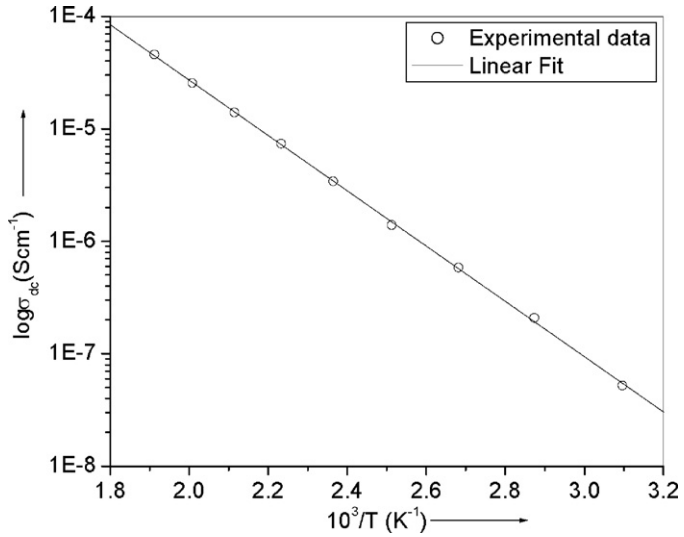

Fig. 5. Variation of σ_{dc} as a function of temperature.

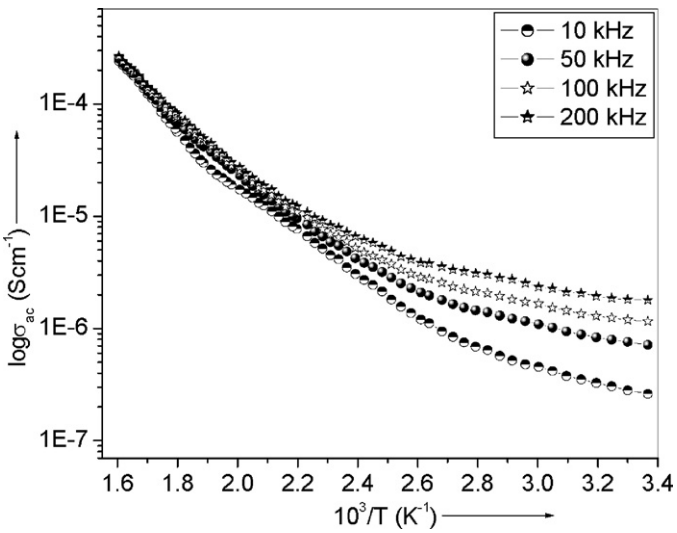

Fig. 7. Temperature dependence of σ_{ac} at some selected frequencies.

rial is a thermally activated process. Similar behavior was shown by $LiFeVO_4$, $LiFe_{1/2}Ni_{1/2}VO_4$ and $LiNiVO_4$ [28,29,40].

The temperature dependence of σ_{ac} at some selected frequencies is shown in Fig. 7. It indicates a progressive rise in σ_{ac} on increasing temperature, which signifies electrical conduction in the material as a thermally activated process. This pattern of variation obeys a relation [$\sigma_{ac} = \sigma_o \exp(-E_a/kT)$], where σ_o is the pre-exponential factor, E_a is the activation energy, k is the Boltzmann constant and T is the absolute temperature [41]. It is observed that the value of E_a decreases with rise in frequency, which is due to the enhancement of electronic jumps between localized states. Similar mechanism was shown by $LiFeVO_4$, $LiFe_{1/2}Ni_{1/2}VO_4$ and $LiNiVO_4$ [28,29,40]. The curves at different frequencies are merging at high temperatures, which may be due to the intrinsic conductivity that takes place in the material at these temperature regions [42].

4. Conclusions

In summary, a $Li(Ni_{7/10}Fe_{3/10})VO_4$ ceramics was prepared by solution-based chemical method. Its X-ray diffraction results reveal an orthorhombic unit cell structure with lattice parameters $a = 8.2272$ Å, $b = 7.0230$ Å and $c = 5.8281$ Å. A field emission scanning electron micrograph indicates a polycrystalline texture of the compound with grains of unequal sizes (~0.1–1.6 μm). Electrical conduction in the material is due to the bulk, grain boundary and polarization effects. A detailed study of electrical conductivity indicates that electrical conduction in the material is a thermally activated process.

Acknowledgement

The author is grateful to the Nanomaterials Laboratory of the Department of Chemistry and Central Research Facility, Indian Institute of Technology, Kharagpur-721302 (W.B.), India, for providing facilities to conduct experiments.

References

[1] S. Satpathy, R.M. Martin, Phys. Rev. B 36 (1987) 7269.
[2] S. Massidda, J. Yu, A.J. Freeman, Phys. Rev. B 38 (1988) 11352.
[3] J. Kim, A. Manthiram, J. Electrochem. Soc. 145 (1988) L53.
[4] N. Hayashi, H. Ikuta, M. Wakihara, J. Electrochem. Soc. 146 (1999) 1351.
[5] T. Nakamura, Y. Yamada, M. Tabuchi, J. Appl. Phys. 98 (2005) 093905.
[6] Y.C. Si, L.F. Jiao, H.T. Yuan, H.X. Li, Y.M. Wang, J. Alloys Compd. 486 (2009) 400.
[7] A. Kuhn, M. Martin, F.G. Alvarado, J. Solid State Chem. 183 (2010) 20.
[8] T.F. Yi, L.J. Jiang, J. Shu, C.B. Yue, R.S. Zhu, H.B. Qiao, J. Phys. Chem. Solids 71 (2010) 1236.
[9] I. Soibam, S. Phanjoubam, L. Radhapiyari, Phys. B 405 (2010) 2181.
[10] J.S. Pena, O. Crosnier, T. Brousse, Electrochim. Acta 55 (2010) 7511.
[11] C.V. Rao, B. Rambabu, Solid State Ionics 181 (2010) 839.
[12] L.H. Chi, N.N. Dinh, S. Brutti, B. Scrosati, Electrochim. Acta 55 (2010) 5110.
[13] M.V. Reddy, A. Levasseur, J. Electroanal. Chem. 639 (2010) 27.
[14] W.M. Tang, S.H. Tang, L. Ping, Sens. Actuators B: Chem. 17 (1994) 109.
[15] F. Gang, C. Huan, H. Sumei, L. Zhiyu, Sens. Actuators B: Chem. 137 (2009) 17.
[16] Y.J. Wei, H. Ehrenberg, K.B. Kim, C.W. Park, Z.F. Huang, C. Baehtz, J. Alloys Compd. 470 (2009) 273.
[17] P.P. Hankare, R.P. Patil, U.B. Sankpal, K.M. Garadkar, R. Sasikala, A.K. Tripathi, I.S. Mulla, J. Magn. Magn. Mater. 322 (2010) 2629.
[18] M. Ram, Phys. B 405 (2010) 602.
[19] J.R. MacDonald, Impedance Spectroscopy: Emphasizing Solid Materials and Systems, John Wiley & Sons, New York, 1987.
[20] Y. Cui, W. Cai, Y. Li, J.Q. Qian, P. Xu, R. Wang, J. Yao, J. Appl. Phys. 100 (2006) 034101.
[21] Y. Cui, L. Zhang, R. Wang, J. Alloys Compd. 428 (2007) 40.
[22] O. Trithaveesak, J. Schubert, C. Buchal, J. Appl. Phys. 98 (2005) 114101.
[23] M. Ram, Solid State Sci. 12 (2010) 350.
[24] S. Tangwancharoen, P. Thongbai, T. Yamwong, S. Maensiri, Mater. Chem. Phys. 115 (2009) 585.
[25] M. Dong, J.M. Reau, J. Ravez, Solid State Ionics 91 (1996) 183.
[26] T. Fehr, E. Schmidbauer, Solid State Ionics 178 (2007) 35.
[27] E. Kazakevicius, A. Urcinskas, A. Kezionis, A. Dindune, Z. Kanepe, J. Ronis, Electrochim. Acta 51 (2006) 6199.
[28] M. Ram, R.N.P. Choudhary, A.K. Thakur, Adv. Appl. Ceram. 105 (2006) 140.
[29] M. Ram, Mater. Chem. Phys. 101 (2007) 455.
[30] M. Ram, Solid State Commun. 149 (2009) 1226.
[31] M. Ram, Mater. Chem. Phys. 109 (2008) 465.
[32] M. Ram, S. Chakrabarti, J. Phys. Chem. Solids 69 (2008) 905.
[33] M. Ram, Curr. Appl. Phys. 10 (2010) 1013.
[34] M. Ram, Phys. B 405 (2010) 2205.
[35] E. Wu, POWD MULT: An Interactive Powder Diffraction Data Interpretation and Indexing Program, Version 2.1, School of Physical Sciences, Flinder University of South Australia, Bardford Park, SA, Australia, 1989.
[36] J. Plocharski, W. Wieczoreck, Solid State Ionics 28–30 (1988) 979.
[37] S. Kumar, K.B.R. Varma, Solid State Commun. 146 (2008) 137.
[38] C.H. Song, H.W. Park, H.W. Choi, M. Kim, Y.S. Yang, J. Korean Phys. Soc. 49 (2006) S465.
[39] A.K. Jonscher, Nature 267 (1977) 673.
[40] M. Ram, Phys. B 405 (2010) 1706.
[41] A. Hassib, A. Razik, Solid State Commun. 147 (2008) 345.
[42] K.S. Rao, D.M. Prasad, P.M. Krishna, B. Tilak, K.C. Varadarajulu, Mater. Sci. Eng. B 133 (2006) 141.